

Temperature Effects on Electrophoresis

Supporting Information

*Anita Rogacs, Juan G. Santiago**

Department of Mechanical Engineering, Stanford University, Stanford, California, 94305

*To whom correspondence should be addressed. E-mail: juan.santiago@stanford.edu. Fax: 650-723-7657

This document contains the following supplementary figures, tables, and information further describing our temperature model:

- List of electrolytes used in this study. Table S-1 includes electrophoretic mobility, dissociation constant, standard molar enthalpy change of ionization, and standard molar heat capacity change of ionization at room temperature, 25°C.
- Predictions for anionic (and cationic) mobility for the solutions described in Table 3 of paper.
- Summary of results of conductivity and pH measurements for additional electrolyte solutions tested to validate our temperature model.
- Additional conductivity and pH measurements for solutions of Tris and boric acid.
- Example simulations of cationic analyte mobilities in various background electrolytes (BGE).

S-1. List of electrolytes used in validation of our temperature model

Table S-1 presents a list of the relevant properties of 13 electrolytes used in this study.

Table S-1. List of chemical species mobility, μ , (in $10^9 \text{ m}^2 \text{ V}^{-1} \text{ s}^{-1}$), $\text{p}K$, standard molar enthalpy of ionization, ΔH° , (in J mol^{-1}) standard molar heat capacity of ionization, ΔC_p° , (in $\text{J K}^{-1} \text{ mol}^{-1}$) values defined at 25°C , as used in main paper.

Name	$\mu(-3)$	$\mu(-2)$	$\mu(-1)$	$\mu(+1)$	$\text{p}K(-3)$	$\text{p}K(-2)$	$\text{p}K(-1)$	$\text{p}K(+1)$	$\Delta H^\circ(-3)$	$\Delta H^\circ(-2)$	$\Delta H^\circ(-1)$	$\Delta H^\circ(+1)$	$\Delta C_p^\circ(-3)$	$\Delta C_p^\circ(-2)$	$\Delta C_p^\circ(-1)$	$\Delta C_p^\circ(+1)$
ACETIC ACID			42.4				4.756				-410				-142	
BORIC ACID			36.5				9.237				13800				-240	
CITRIC ACID	74.4	54.7	28.7		6.396	4.761	3.128		-3380	2230	4070		-254	-178	-131	
HEPES			23.5				7.564				20400				47	
HYDROCHLORIC ACID			79.1				-2				0				0	
MOPS			26.9				7.184				21100				25	
PHOSPHORIC ACID	71.5	61.4	34.6		12.35	7.198	2.148		16000	3600	-8000		-242	-230	-141	
BISTRIS				26				6.484			28400				27	
ETHANOLAMINE				44.3				9.498				50520				26
HISTIDINE			28.3	28.8			9.34	6.07			43800	29500			-233	176
POTASSIUM				76.2				13				0				0
SODIUM				51.9				13.7				0				0
TRIS				29.5				8.072				47450				-59

S-2. Predictions for anionic (and cationic) mobility for the solutions described in Table 3 of paper

In the main paper, we validated our MATLAB-based tool for Simulation of Temperature Effects on ElectroPhoresis (STEEP) using conductivity and pH measurements in the temperature range of 25°C to 70°C for electrolyte solutions listed in Table 3. In Figure 4 of paper, we plot the conductivity as a function of temperature, T , with respect to conductivity evaluated at the reference temperature, θ , as follows: $\sigma(T)/\sigma(\theta)$, where $\theta = 25^\circ\text{C}$. A detailed discussion on the underlying physical phenomena governing the observed conductivity behavior of ethanolamine-borate solution is presented as the description of Figure 1 of the paper. Here, we present similar discussions on the remaining three buffers listed in Table 3.

Figures S-1, S-2, and S-3 show plots of the effective mobility of the participating anion (Figure S-1, we also plot cation mobility) for temperatures from 25°C to 70°C, with respect to its effective mobility at the reference temperature, $\theta = 25^\circ\text{C}$, as follows: $\mu_{-}(T)/\mu_{-}(\theta)$ (the subscript indicates an anion). The curves associated with our full temperature model (including all effects considered here) are labeled “Current”. In the insets of these figures, we show predictions of our full temperature model for the anion and cation p*K*s and solution pH as functions of temperature.

As with Figures 1-3 of the main paper, these figures include additional curves which we use to demonstrate the effect of individual physical phenomena described in the Table 1 of paper. Recall, the simplest model, ‘W’, uses only the Walden’s viscosity correction term, α , to evaluate effective mobility at elevated temperature. Model ‘SSC’ captures the temperature dependence of limiting ionic mobility due to changes in solvation, Model ‘ISC’ quantifies the temperature dependence of the extended Onsager-Fuoss and the extended Debye-Huckel theory, and Model ‘p*K*C’, captures the temperature effects on the degree of ionization. If one of these physical phenomena has no temperature contribution to mobility (other than a Walden type behavior), its corresponding limiting model overlaps with model ‘W’; in such cases, we chose not to plot the curve.

Figure S-1 shows predictions for the second electrolyte in Table 3, which is composed of 50 mM potassium citrate ($\text{p}K_{-3} = 6.396$, $\text{p}K_{-2} = 4.761$, $\text{p}K_{-1} = 3.128$) mixed with 200 mM Bis-tris ($\text{p}K = 6.484$). Citric acid is trivalent and is therefore very sensitive to ionic strength effects. Further, potassium is a small ion whose hydration changes with temperature. We also added weak Bis-tris to increase the pH. We chose this solution as a large difference between the pH and citrate p*K*s ensures that citrate remains fully ionized for all temperatures. This enables the isolation of two temperature related phenomena: ionic strength effects on citrate ion mobility (right plot) and ion solvation effect on the potassium ion mobility (left plot). Note that, since $\text{pH} > \text{p}K_{\text{Bis-tris}} - 2$, Bis-tris is practically neutral and has virtually zero effective mobility. Bis-tris therefore has negligible contribution to solution ionic strength and conductivity. This solution is an interesting example of ionic strength and solvation effects, but it is a poor buffer with buffering capacity of only ~0.6 mM.

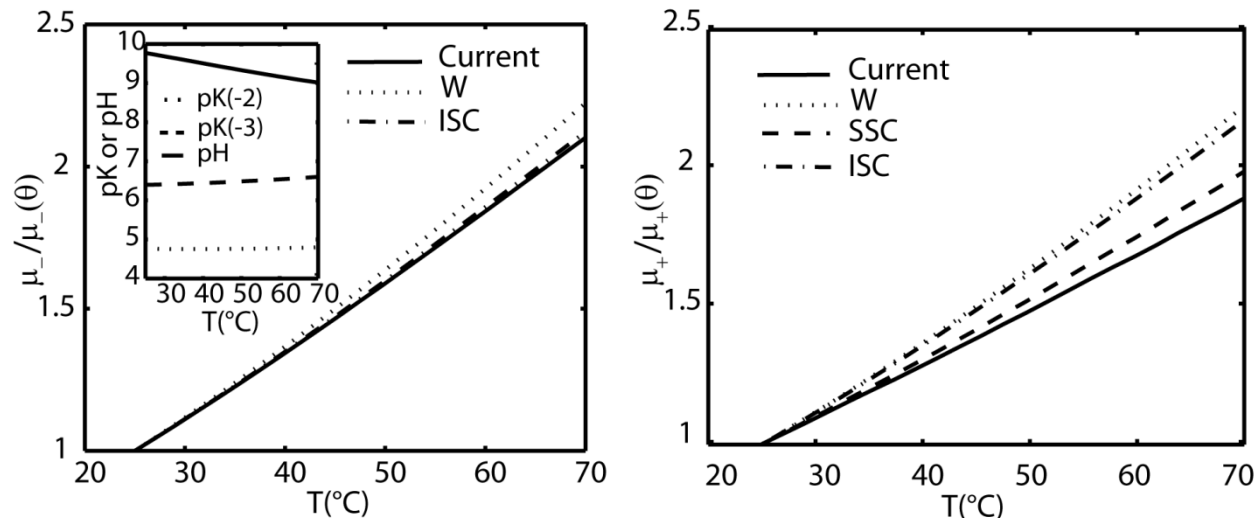


Figure S-1. Prediction of anionic (citrate) and cationic (potassium) mobilities in an electrolyte solution composed of 50 mM potassium citrate ($pK_3 = 6.396$, $pK_2 = 4.761$, $pK_1 = 3.128$) mixed with 200 mM Bis-tris ($pK = 6.484$) (Solution 2, in Table 3 of paper). Left plot shows the predicted electrophoretic mobility of a trivalent ion, citrate. In the inset, we show only the pK of the trivalent and divalent anion of citric acid, which lie far from the solution pH , indicating no change in degree of ionization. Thus we can attribute the change in the effective mobility of citrate to temperature variation of ionic strength correction terms. Right plot shows the predicted electrophoretic mobility of a monovalent cation, potassium. The simple ‘SSC’ model is fairly accurate here which suggests that the dominant source of the non-viscosity related temperature dependence is due to the change in the hydration shell of the potassium ion. The residual deviation of ‘SSC’ from the ‘Current’ solution is due to the temperature dependence of ionic strength correction, captured by ‘ISC’. Limiting models ‘SSC’ and ‘pKC’ (and ‘pKC’ on the left plot) are not plotted as they nearly perfectly overlap the W curve.

Figure S-2 shows a weak-electrolyte buffer composed of 30 mM Tris and 30 mM HEPES (the third solution in Table 3). Here, the model predicts a shallow, linear anionic mobility curve. Limiting model pKC matches well with the comprehensive model (Current), suggesting that the temperature induced decrease in degree of ionization is the primarily the source of the observed mobility behavior. This conclusion is supported by the pK and pH trend shown in upper inset which show that the temperature dependence of Tris pK is much stronger than that of HEPES. At room temperature, the anion and cation pK s are close to and bound the solution pH . As temperature is increased, the buffer pH decreases faster than the pK of HEPES. This decreases the ionization of HEPES ion, thereby decreasing its effective mobility.

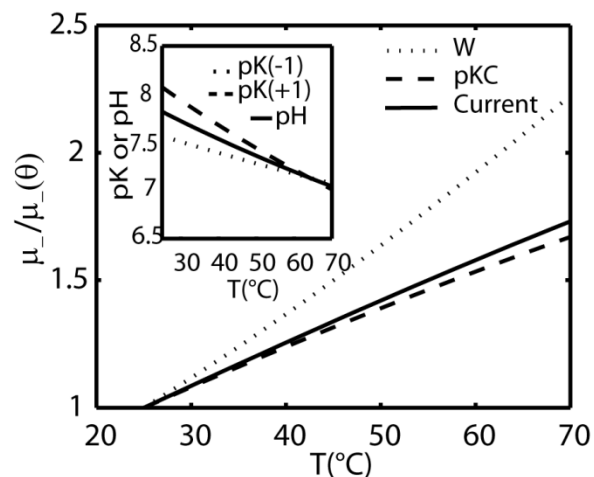


Figure S-2. Predicted electrophoretic mobility versus temperature for HEPES (anion) in the solution of 30 mM Tris and 30 mM HEPES (Solution 3, in Table 3 of main paper). Increase in temperature results in a strong drop in the pK of Tris and a moderate drop in the pK of HEPES, resulting in an overall decrease in pH (inset). Here, the most prominent contribution to anion mobility is due to the sharp reduction in degree of ionization of HEPES (hence the proximity of ‘pKC’ model to ‘Current’). Predictions based on Walden rule here overestimate the anion mobility by 30% at 70°C. Limiting models ‘SSC’ and ‘ISC’ are not plotted as they nearly perfectly overlap the W curve.

Figure S-3 shows a weak-electrolyte buffer composed of 30 mM Tris and 15 mM acetic acid (Solution 4 in Table 3). Here, the comprehensive model (Current) tracks model ‘W’ closely, suggesting temperature effects on ion solvation, ionic strength correction, and degree of ionization are insignificant. The latter conclusion is supported by the pK and pH trend shown in upper inset of Fig. S-3. Tris is included at twice the concentration of acetic acid, so the solution pH is dominated the $pK(T)$ function of Tris. The large difference (>2 units for all temperatures) between the acetate pK and solution pH ensures the acetate remains fully ionized for all temperatures. In this electrolyte solution, the mobility of acetate can be estimated by correcting for changes in viscosity of water alone.

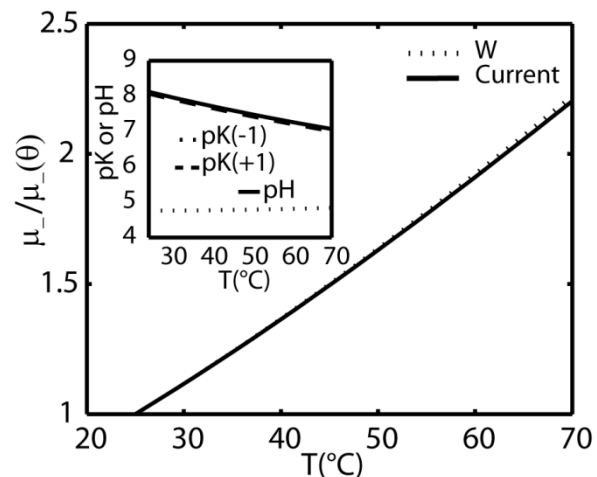


Figure S-3. Predicted electrophoretic mobility versus temperature of acetate (anion) in a solution containing 30 mM Tris and 15 mM acetic acid (Solution 4, in Table 3 of MS). Here, ionic strength of solution containing cation (Tris) and titrant (acetic acid) are determined by the molarity of the fully-ionized acetic acid. While the pH varies with temperature dictated by the $pK(T)$ function of the Tris, the large difference (>2 units for all T) between acetate pK and solution pH ensures that acetic acid remains fully ionized. Therefore, the acetate mobility predictions based on Walden's rule estimate anion mobility fairly accurately, within $\sim 4\%$. Limiting models 'SSC', 'ISC', and 'pKC' are not plotted as they nearly perfectly overlap the W curve.

S-3. Summary of conductivity measurements for six additional electrolyte solutions and comparison with temperature model

As part of our study, we experimentally quantified conductivity and pH as a function of temperature for a total of ten example electrolyte solutions. In the main paper, we discuss in detail four of these. The data of in Table S-2 is a compact summary of our conductivity and pH measurements for six additional electrolyte solutions. Following the experimental procedure described in the paper, we recorded pH and conductivity values of solution listed in Table S-2 at 25°C and 70°C. With the sole exception of Tris-borate buffer, the conductivity and pH predictions agreed to measured values within 4% (corrected for room temperature offset as described in Results and Discussion of main paper) and 0.2 pH units. Out of the 10 solutions we explored, we found surprisingly large discrepancies between the model and experiments only for two solutions with the particular combination of Tris and boric acid. For 10 mM Tris and 10 mM boric acid solution, pH predictions were different by 0.10 and 0.18 pH units, and conductivity predictions were different by 14% and -17%, respectively for temperatures 25°C and 70°C. The discrepancy was more severe for 100 mM Tris and 100 mM boric acid solution, where pH predictions were off by 0.34 and 0.32 pH units and conductivity prediction were off by 68% and -18%, respectively for 25°C and 70°C. We discuss this outlier case further in the next section, but note there that simple models cannot predict even the room temperature behavior of this electrolyte combination.

Table S-2. Summary of predictions and measurements of pH and conductivity for six additional electrolyte solutions at temperatures 25°C and 70°C.

Composition		pH (T=25°C)				pH (T=70°C)			
		pH _{exp}	pH _{th}	σ_{exp} ($\mu\text{S/cm}$)	σ_{th} ($\mu\text{S/cm}$)	pH _{exp}	pH _{th}	σ_{exp} ($\mu\text{S/cm}$)	σ_{th} ($\mu\text{S/cm}$)
30 mM Bis-tris	30 mM MOPS	6.75	6.83	466	444	6.19	6.25	945	868
30 mM NaOH	20 mM phosphoric acid	7.22	6.98	2620	2463	7.21	6.99	5780	5358
20 mM L-histidine	20 mM acetic acid	5.34	5.41	1017	1013	5.03	5.07	1795	1796
100 mM Tris	50 mM HCL	8.19	8.15	4470	4527	7.12	7.10	8970	9378
10 mM Tris	10 mM boric acid	8.55	8.65	115	131	7.82	8.00	142	118
100 mM Tris	100 mM boric acid	8.31	8.65	749	1258	7.68	8.00	1414	1161

S-4. Additional conductivity measurements for Tris-boric acid buffer

Of the ten electrolyte solutions we explored in detail, we observed substantial discrepancies between model and measurements only for solutions which specifically combine Tris and boric acid (see Table S-2). Interestingly, conductivity and pH temperature trends (and absolute values) for these same electrolytes are well predicted by our model when they are each paired with other ions (e.g.: ethanolamine and boric acid Tris-HEPES, Tris-HCl, and Tris-acetate).

In an attempt to understand this discrepancy, we further examined the conductivity trend with temperature for equimolar Tris and boric acid solutions. In Figure S-4, we plot the measured and predicted conductivity ratio and the $\log_{10}f$ factor for 10 mM and 100 mM solutions in 5°C increments. As shown in the top inset, at lower ionic strength, conductivity is concave down and parabolic similar to the predicted anion mobility curve shown for ethanolamine and boric acid buffer (Fig. 4 of paper). Our theory predicts that the change in degree of ionization of boric acid has significant contribution to the conductance of this solution, which is qualitatively confirmed at lower ionic strength. However, the model grossly overpredicts the magnitude of this contribution at higher ionic strength.

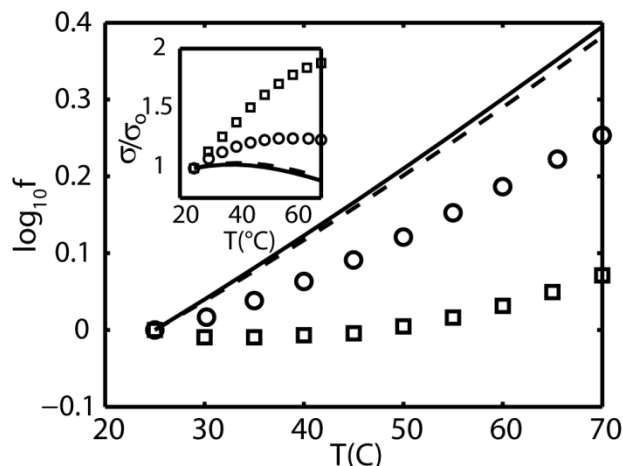


Figure S-4. Theory curves together with respective conductivity (σ) measurements (raw data) for 10 mM Tris and 10 mM boric acid (solid line and ‘○’), and for 100 mM Tris and 100 mM boric acid (dashed line and ‘□’). The factor f is defined as $\sigma(\theta)\eta(\theta)/\sigma(T)\eta(T)$, where $\theta = 25^\circ\text{C}$, and η is dynamic viscosity. The difference between model prediction and measured values is very significant for the particular combination of Tris and boric acid. We also observed a large discrepancy in the conductivities measured room temperature (see Table S-2 and Figure S-5).

We further examined the room temperature behavior of this solution, by preparing an equimolar solution of 150 mM Tris and boric acid, and measuring pH and conductivity at multiple concentrations during the dilution process. Figure S-5 shows large deviation between the data and the corresponding theory. Recall, our theory includes the Onsager-Fuoss correction on limiting mobilities, and the Debye-Huckel correction of ionic activities, yet our predictions do not capture the observed ionic strength dependence. Thus, we hypothesize that the observed conductivity and pH trend is associated with product(s) of a side reaction or complexation between boric acid and Tris. This hypothesis is strongly supported by the work of Michov, who

showed that Tris-borate buffers contain a cyclic complex compound of betainic structure therefore they do not obey the Henderson-Hasselbalch equation (see main paper for reference).

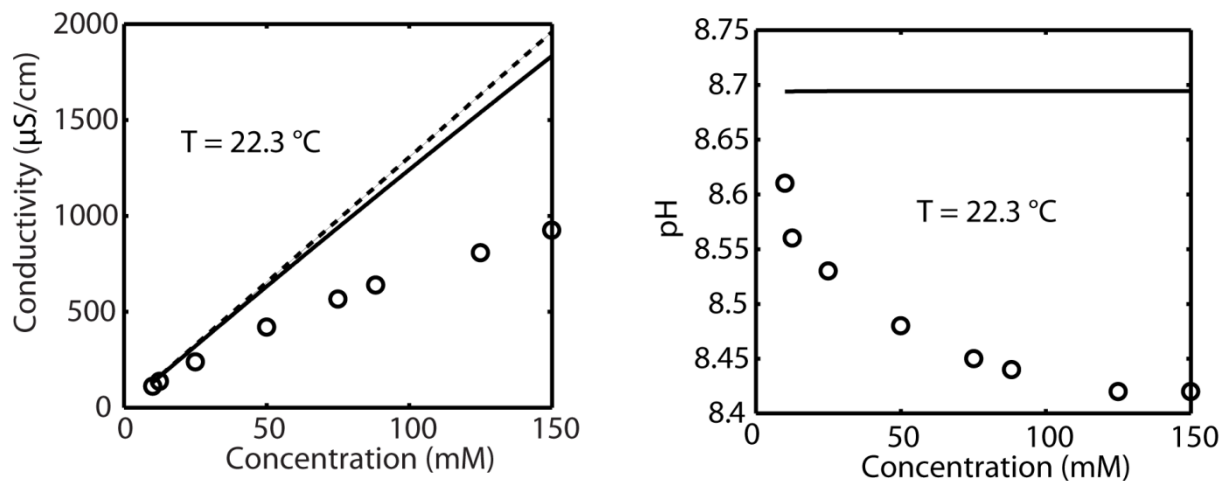


Figure S-5. Room temperature (22.3°C) prediction and measurements (\circ) of conductivity and pH of equimolar Tris and boric acid solution in the range of 10 mM to 150 mM concentration. For comparison, we present the (full) model with (solid line) and without (dashed line) ionic strength correction. The ionic strength effects on activity coefficients are weak (dashed line and solid line for pH predictions overlap). The large deviation of model from data, and the observed strong dependence of conductivity and pH on ionic strength suggest solutions of Tris and boric acid are strongly influenced by the presence of other reactions or complexation between the Tris and boric acid, which are not captured by our model.

S-5. Three distinct mobility trends associated with a single cation (Bis-tris), in three different background buffers

We explored the temperature trends of Bis-tris mobility in three background buffers (Fig. S-6). We offer this as an interesting example of the very different and sometimes counterintuitive temperature trends which a single species can exhibit in different solutions. Table S-3 summarizes the three buffers we considered.

Table S-3. Three buffers chosen to demonstrate the different cationic mobility trends exhibited by Bis-tris as temperature is increased

Analyte	Buffer	pH _{20°C}	ΔpH _{20°C-80°C}	Notes
100 μM Bis-tris pK ₊₁ = 6.484	Buffer A			
	10 mM phosphoric acid 15 mM NaOH	7.04	0.03	Mobility decreases w/ increasing temperature
100 μM Bis-tris pK ₊₁ = 6.484	Buffer B			
	15 mM HCL 30 mM imidazole	7.15	1.10	Mobility follows viscosity line (Walden's predication in this case is fairly accurate)
100 μM Bis-tris pK ₊₁ = 6.484	Buffer C			
	25 mM Tris 20 mM Acetic Acid	7.67	1.33	Mobility increases steeply with temperature.

The observed mobility trends are all due to temperature induced changes in degree of ionization of the analyte. This particular cation has a pK within 2 units of the pH of each of the selected buffers. Bis-tris also has a steep, negative value of dpK/dT. The mobility of Bis-tris therefore displays the following properties:

- decreases if the solution dpH/dT > dpK/dT. (Buffer A).
- increases with a slope predicted by the change in viscosity if dpH/dT = dpK/dT. (Here, Buffer B dpH/dT is slightly smaller than the Bis-tris dpK/dT, so the mobility of Bis-tris increases slightly above the mobility predicted by Walden's rule)
- increases sharply (to mobilities well above the values estimated by Walden's rule) if dpH/dT < dpK/dT (Buffer C).

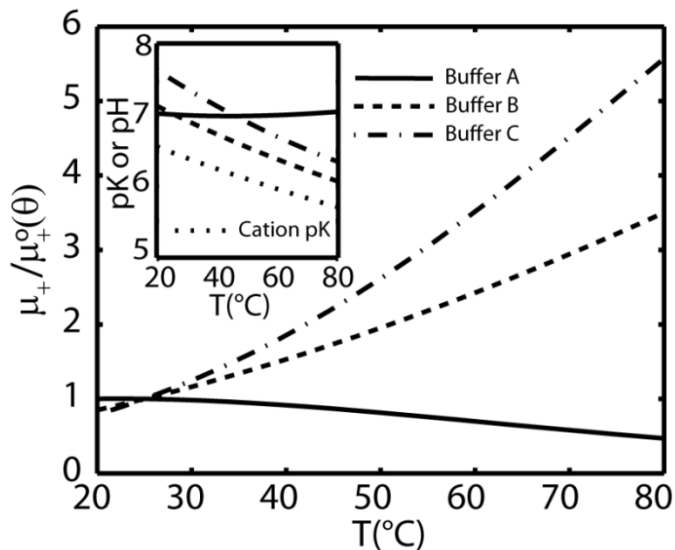


Figure S-6. Predicted mobility of cationic analyte (100 μM Bis-tris) in three example electrolyte systems. The main plot shows the effective mobility of Bis-tris at temperature T , normalized by its mobility at the reference temperature θ for three different buffers (A, B, C) listed in Table S-3. The inset shows the $\text{pH}(T)$ of each background buffer and the $\text{pK}(T)$ of Bis-tris. In all cases, buffer pH is within 2 units from the analyte pK . In Buffer A, at room temperature, Bis-tris pK is ~ 1 unit below the pH , causing Bis-Tris to be poorly ionized. Over 60°C increase in temperature, the Bis-tris pK decreases further below the pH of Buffer A, resulting in a reduction in ionization so severe, that it overcomes the effect of decreasing water viscosity. pH of Buffer B and C both start above the Bis-Tris pK , making Bis-tris poorly ionized in these buffers as well. However, as temperature increases, the pH of both buffers approach the pK of Bis-tris, causing an increase in dissociation and effective mobility.

S-6. Three analytes with distinct mobility trends in a single background electrolyte buffer

We explored the temperature trends of the mobility of three model analytes (two cations and one ampholyte) in a single background buffer (Fig. S-7). As in the last section, we offer this as an interesting example of the very different and sometimes counterintuitive temperature trends which a species can exhibit. Table S-4 summarizes the three analytes considered as well as the example background buffer.

Table S-4. Properties of three electrolyte species whose mobility temperature trend we explored in a single background buffer containing phosphoric acid and NaOH. The three species of interest are ethanolamine, Bis-tris, and L-histidine.

Analyte	Buffer	Notes
100 μ M ethanolamine $pK(+1) = 9.498$		Mobility increase follows Walden's prediction
100 μ M Bis-tris $pK(+1) = 6.484$	10 mM phosphoric acid 15 mM NaOH $pH_{20^{\circ}C} = 7.04$ $\Delta pH_{20^{\circ}C-80^{\circ}C} = 0.03$	Mobility decreases slightly relative to room temperature value
100 μ M L-histidine $pK(-1) = 9.34$ $pK(+1) = 6.07$		L-histidine is an ampholyte, so its mobility decreases to zero and changes sign within a 60°C temperature change.

Again, here, the observed mobility trends are all due to temperature-induced changes in degree of ionization of the analyte. In this particular case, the buffer pH is held constant ($dpH/dT \sim 0$), so the mobility of the analyte

- increases roughly according to Walden's rule prediction if $pH < pK - 2$. For example, ethanolamine pK at room temperature is over 2 units above the pH of solution, so its ionization is not affected by the temperature dependence of its pK at most temperatures.
- decreases if $dpH/dT > dpK/dT$ and $pK - 2 < pH < pK + 2$. For example, the pK of Bis-tris is in close proximity to the pH of the solution, and its decreasing pK results in a reduction of its degree of ionization and therefore its effective mobility.
- decreases to zero and can change sign if the analyte is an ampholyte with room temperature values of pK which meet the following condition: $pK_{+1} < pH < pK_{-1}$ and $dpH/dT > dpK/dT$.

These complex and sometimes counterintuitive temperature trends exhibited by common buffer species highlight the importance of high fidelity simulations for buffer design and the optimization of a wide range of electrophoresis processes.

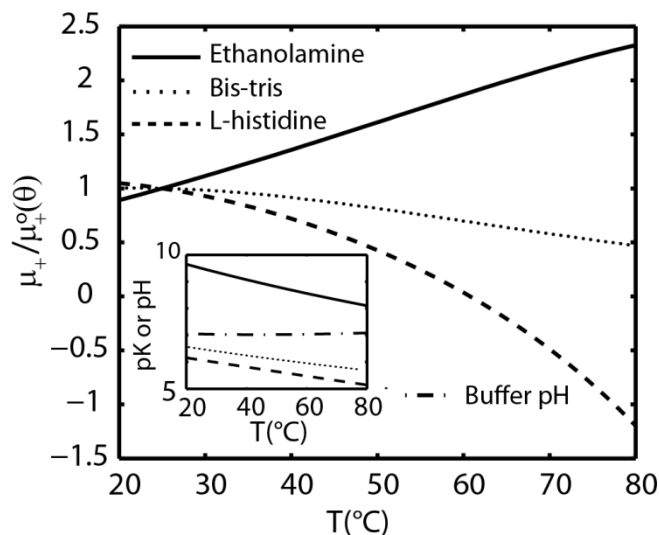


Figure S-7. Predicted mobility of cationic analytes (100 μM ethanolamine, 100 μM Bis-tris and 100 μM L-histidine). Each model analyte is considered in a solution of a single background buffer with pH which is insensitive to temperature. (See Table S.4 for electrolyte composition, and analyte properties) The main plot shows the effective mobility of the three analytes as a function of temperature T , normalized by their mobility at the reference temperature, θ . The buffer pH, and its proximity to the analytes' pK s, is shown in the inset. Between 20 $^{\circ}\text{C}$ and 50 $^{\circ}\text{C}$, pK of ethanolamine stays 2 units above the solution pH, keeping this analyte completely ionized. For this temperature range, the mobility of ethanolamine monotonically increases with temperature according to Walden's rule. Above 50 $^{\circ}\text{C}$ there is slight reduction in its ionization, reflected by a small change in the slope of mobility with temperature. In the remaining two cases, the buffer pH is within ~ 2 units of the analyte pK s. The most interesting of the two cases is of L-histidine, which is an ampholyte with $pK_{-1}= 9.34$ and $pK_{+1}= 6.07$. The pK values have similar temperature dependence. As temperature increases, the basic group of L-histidine gradually neutralizes, while the acidic group becomes more ionized. At about 60 $^{\circ}\text{C}$ the effective mobility of L-histidine is zero and becomes negative at higher temperatures.